

皮秒绿激光修锐青铜基金刚石砂轮损伤规律与机制

周远航¹, 张健^{1,2*}, 冯爱新^{1,2}, 尚大智¹, 陈云³, 唐杰¹, 杨海华¹

¹ 温州大学机电工程学院, 浙江 温州 325035;

² 浙江省激光加工机器人重点实验室, 浙江 温州 325035;

³ 成都工具研究所有限公司, 四川 成都 610500

摘要 为探究皮秒绿激光修锐青铜基金刚石砂轮的工艺规律与机制, 实现青铜基体的选择性定量去除。首先采用 10 ps 绿激光作用于青铜/金刚石, 利用 S-on-1 损伤测定法标定损伤阈值, 确定皮秒激光修锐青铜/金刚石砂轮的最佳工艺参数范围。然后对青铜/金刚石砂轮表面进行修锐, 通过激光共聚焦显微镜及其软件表征修锐表面形貌与表面粗糙度, 探究激光峰值功率密度、重复频率、扫描次数对修锐效果的影响规律。结果表明, 皮秒绿激光对青铜基体的去除机制主要为气化去除, 很大程度上避免了金刚石磨粒的碳化, 即使在高重复频率下, 也无明显的热积累特征。在脉宽为 10 ps、重复频率为 400 kHz 条件下, 青铜基体与金刚石磨粒的损伤阈值分别为 $1.23 \times 10^9 \text{ W/cm}^2$ 、 $3.71 \times 10^{11} \text{ W/cm}^2$, 两者相差两个数量级, 青铜基体的选择性微量去除选择范围较宽, 可通过调节峰值功率密度有选择性地去除基体, 通过调节扫描次数定量去除基体。因此, 采用皮秒绿激光可以选择性定量去除青铜基体且较好地保证金刚石磨粒的完整性。

关键词 激光加工; 皮秒激光; 青铜基金刚石砂轮; 激光修锐; 损伤阈值

中图分类号 TG74+3

文献标志码 A

doi: 10.3788/CJL202148.0602116

1 引言

近年来, 以光学玻璃、工程陶瓷与硬质合金等硬脆材料制成的工程构件在航空航天、国防、天文观测等尖端领域的应用愈加广泛。超硬磨料砂轮作为硬脆材料精密、超精密磨削加工的主要工具, 其应用日益广泛、用量急剧增加^[1-2]。其中青铜基金刚石砂轮因其具有极高的硬度与抗磨能力, 已经成为硬脆材料磨削加工的理想工具。金刚石砂轮一般通过烧结、电镀或钎焊制备而成, 在其制备及使用过程中, 需要进行修整才能保持其几何形状与优越的使用性能^[3]。但其超硬特性使得磨钝后存在修整难度大、耗时长、修整工具损耗大等问题, 在一定程度上严重影响了使用性能^[4]。

金刚石砂轮修整通常包括整形和修锐两个阶段^[5-6], 整形是指微量切削砂轮工作表面, 使砂轮获

得精确的几何形状; 修锐是指去除金刚石磨粒间部分结合剂, 使金刚石磨粒突出, 形成切削刃, 同时具有一定的容屑空间。目前国内外学者通常采用传统的机械修整法与电加工等方法对该类砂轮进行修整, 存在修整工具损耗大、修整效率低、环境污染重等弊端^[7-8]。激光修整法是近年来快速发展起来的一种绿色新工艺^[9-11], 一般分为切向整形和径向修锐, 作为一种非接触式修整方法, 完全避免了传统修整方法带来的机械损伤与修整工具的损耗, 具有高效、环保、适用性广、可控性高等显著优势。

激光修锐的实质就是利用高能聚焦光束沿砂轮径向方向辐照其工作表面, 利用激光烧蚀的热力学效应将砂轮表面的青铜结合剂选择性微量去除, 而对磨粒不造成损伤, 使磨粒突出黏合剂适当的高度, 从而沿砂轮表面形成均匀排列的切削刃与微米级烧蚀坑。目前, 国内外学者已经开展了较为广泛的研

收稿日期: 2020-06-28; 修回日期: 2020-08-07; 录用日期: 2020-10-10

基金项目: 浙江省自然科学基金(LY20E050026)、浙江省一般科研项目(Y201839918)、温州市科技计划项目(G20190011,ZG2019002)

* E-mail: zhangjian200623@sina.com

究,大多采用传统长波长连续、毫秒与纳秒红外激光,该类传统激光的去除机制为熔化气化去除,这种去除机制产生的热效应易使金刚石碳化,产生石墨化变质层,使得砂轮表面疲劳强度和硬度显著降低,导致磨削性能下降。Chen 等^[12]、郭晓光等^[13]、Deng 等^[14]的研究表明,在 800 ℃ 空气环境中青铜基体中铁族金属、铜及其氧化物可以活化金刚石中的碳原子或为其提供活性氧,从而促进金刚石的石墨化转变。由此可见,激光修锐青铜基金刚石砂轮的关键在于基体的选择性定量去除并尽量避免金刚石石墨化,这一关键问题也成为了制约激光修锐工艺工程化应用的技术瓶颈。

随着激光光源技术的快速发展,短波长皮秒、飞秒激光以其“电子态”冷加工的技术优势不断向各领域渗透,并得以应用^[15-16]。研究结果初步表明^[17-19],采用皮秒激光修整金刚石砂轮时未发生明显的石墨化转变,同时很大程度上抑制了金刚石磨粒因为高温而产生的热损伤。另外,考虑到铜基材料对绿激光有较高的吸收率^[20-21],也有利于青铜基金刚石砂轮的选择性定量去除。

因此,本文采用皮秒绿激光对青铜基金刚石砂轮进行径向修锐,研究皮秒绿激光作用青铜/金刚石复合材料的损伤特性与规律。依据青铜基体与金刚石损伤差异确定最佳工艺参数范围,探究激光峰值功率密度、重复频率、扫描次数对修锐效果的影响规律与损伤机制。

2 试验条件与方法

2.1 试验设备及方法

试验材料为工程常用直径 125 mm、厚度 20 mm 的青铜基金刚石砂轮,如图 1 所示。其中青铜基体由体积分数约 70% 的 Cu 与约 25% 的 Sn 经烧结而成,此外加入了少量的钴粉、镍粉提高其强度、热稳定性、耐磨性及耐腐蚀性;磨粒采用粒度为 80 目(粒径 180~212 μm)的单晶金刚石,约占砂轮总体积分数的 25%;该材料由成都工具研究所有限公司提供。



图 1 青铜基金刚石砂轮

Fig. 1 Bronze-based diamond grinding wheel

试验设备采用超快激光精密加工系统,如图 2 所示。采用 TruMicro5050 型皮秒激光器,能产生最大单脉冲能量为 500 μJ,脉冲重复频率为 100~1000 kHz、脉宽为 10 ps、基频为 1030 nm 的激光,经倍频器后转换(转换效率约为 50%)为输出波长为 515 nm 的绿激光,然后经光学传输系统($f\text{-}\theta$ 镜,

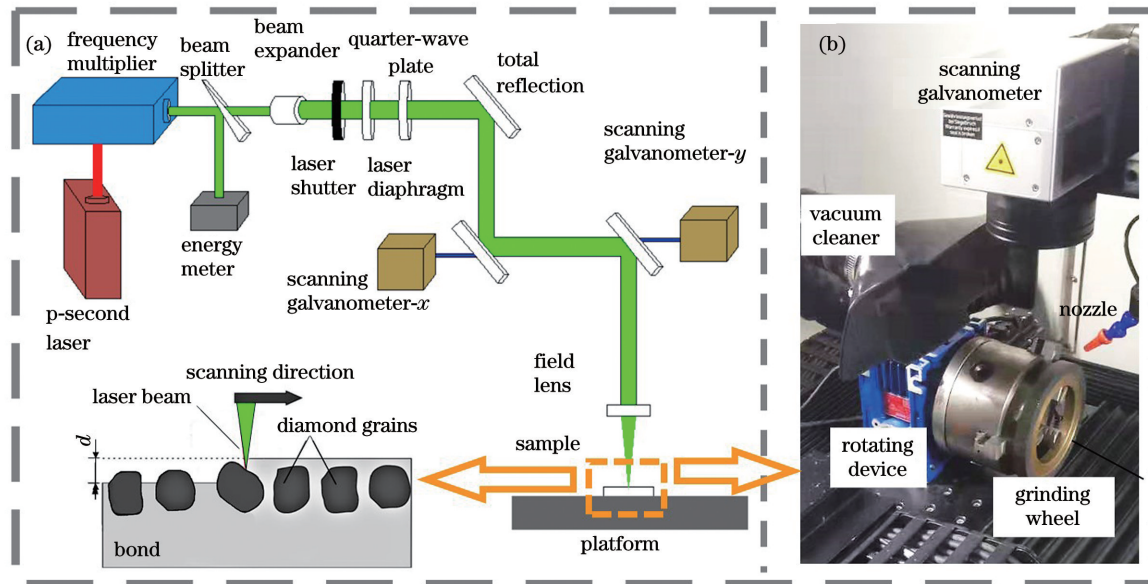


图 2 试验方法与原理。(a)超快激光精密加工系统原理图;(b)修锐实物图

Fig. 2 Experimental method and principle. (a) Schematic diagram of ultrafast laser precision machining system;

(b) factual picture of sharpening

$f=100\text{ mm}$)聚焦至安装在三爪卡盘上的金刚石砂轮表面,聚焦光斑呈高斯分布、直径约为 $30\text{ }\mu\text{m}$ 。为保证径向修锐工艺的顺利实施,激光束沿砂轮法向入射,即垂直于砂轮表面切向面。砂轮由伺服电机带动三爪卡盘匀速转动,其轴向进给由下方精密加工平台实现[图2(b)]。

研究结果表明^[22],影响脉冲激光修锐的主要参数之一为激光峰值功率密度,峰值功率密度在一定程度上决定着砂轮表面的热积累程度与材料去除机制。因此,试验首先采用S-on-1损伤测定法^[23-24],利用不同功率密度的皮秒激光对样品进行多脉冲辐

照来标定损伤阈值,每个功率密度辐照16个测试点,考虑到脉冲激光的能量累积效应^[25],每个测试点辐照 4×10^5 个脉冲,测试点的移动与定位由下方精密加工平台控制。试验完成过后,按照2.2节中所述方法获得损伤阈值。

依据所获得的损伤阈值,利用控制变量法(峰值功率密度、脉冲重复频率、扫描次数),选取较佳工艺参数进行修锐试验。其中,重复频率与扫描次数由控制软件直接设定,峰值功率密度由软件设置的平均功率与重复频率共同设定,试验参数如表1所示。

表1 激光修锐工艺参数表

Table 1 Laser sharpening process parameter table

Item	No.	P /W	F /kHz	Number	Peak power density /(W·cm ⁻²)
Power density	1	5	400	100	1.77×10^{11}
	2	10	400	100	3.54×10^{11}
	3	15	400	100	5.31×10^{11}
	4	20	400	100	7.07×10^{11}
Pulse repetition frequency	1	5	200	100	3.54×10^{11}
	2	10	400	100	3.54×10^{11}
	3	15	600	100	3.54×10^{11}
Scanning times	1	10	400	50	3.54×10^{11}
	2	10	400	100	3.54×10^{11}
	3	10	400	150	3.54×10^{11}

2.2 测试表征方法

利用三维激光共聚焦显微镜(OLS4100,OLYMPUS公司,日本)观察样品表面损伤情况与修锐效果,采用S-on-1损伤测定法^[23-24],青铜基体依据损伤波纹的连续性标定测试点损伤情况,统计各功率密度下的损伤概率。若测试点损伤区域呈连续性明亮周期波纹,则定义该点为已损伤;若损伤区域呈间断性灰暗波纹,则不计损伤,如图3所示。金刚石则依据损伤凹坑直径大小来定义损伤以及未损伤。然后利用Matlab软件进行最小二乘法计算,对损伤概率非100%的测量点进行线性拟合,获得青铜基体与金刚石各自的损伤阈值曲线。

修锐完成后,首先通过共聚焦显微镜获得修锐区二维与三维形貌图,分别对整体修锐效果与局部磨粒损伤及容屑空间进行分析;并通过显微镜自带LEXT软件,计算面粗糙度 S_a ,综合评估修锐效果。

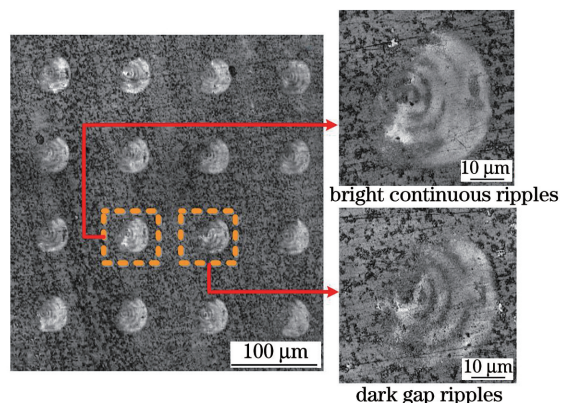


图3 青铜基体损伤概率

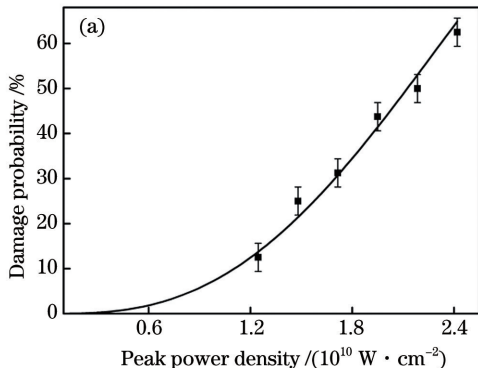
Fig. 3 Damage probability for bronze matrix

3 分析与讨论

3.1 损伤阈值与损伤形貌特征分析

激光修锐金刚石砂轮时,合理标定基体与金刚石各自的损伤阈值是实现材料选择性微量去除与工

艺优化的先决条件。图4为400 kHz皮秒绿激光辐



照下青铜基体与金刚石各自的损伤阈值曲线。

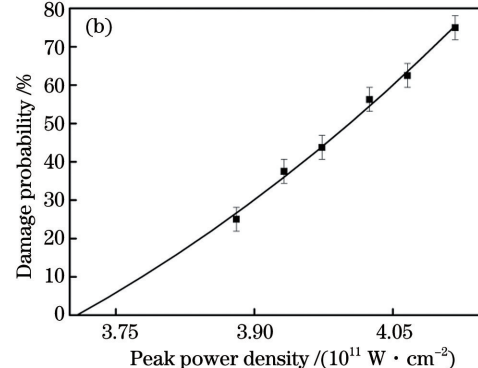


图4 青铜基体与金刚石多脉冲损伤阈值拟合结果。(a)青铜基体损伤阈值拟合曲线;(b)金刚石损伤阈值拟合曲线

Fig. 4 Multi-pulse damage threshold fitting results of bronze matrix and diamond. (a) Fitting curve for bronze matrix damage threshold; (b) fitting curve for diamond damage threshold

由图4可知,10 ps绿激光辐照条件下,青铜基体损伤阈值约为 $1.23 \times 10^9 \text{ W/cm}^2$,金刚石损伤阈值约为 $3.71 \times 10^{11} \text{ W/cm}^2$,两者相差两个数量级,损伤概率随激光功率密度几乎呈线性增大。由图4(a)可知,激光修锐青铜基金刚石砂轮的功率密度数量级在 $2.7 \times 10^{10} \sim 3.7 \times 10^{11} \text{ W/cm}^2$ 范围内较为合适。在实际修锐过程中,在固定脉冲重复频率条件下,通过平均功率与扫描速度的合理匹配,可以有选择性地定量去除青铜基体而不造成金刚石损伤或微量损伤。

图5和图6分别为 $3.54 \times 10^{11} \text{ W/cm}^2$ 功率密度条件下,青铜基金刚石砂轮修锐前后的表面形貌与横截面粗糙度曲线。由图5(a)可知,初始砂轮表面较为平整,经计算面粗糙度 S_a 约为 $29.78 \mu\text{m}$,金刚石磨粒不突出,且凹坑数量少,容屑空间小。由图6可以看出,原始砂轮表面的波峰与波谷的平均高度差在 $66.62 \mu\text{m}$ 左右,粗糙度曲线变化较为平缓,表明金刚石磨粒间有大量的青铜基体包裹,且容

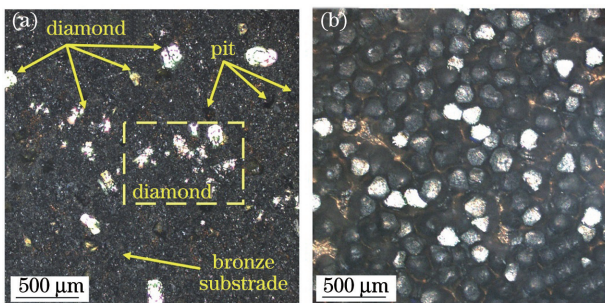


图5 青铜基金刚石砂轮修锐前后的表面形貌。(a)修锐前;(b)修锐后

Fig. 5 Surface morphology of bronze-based diamond grinding wheel before and after sharpening.
(a) Before sharpening; (b) after sharpening

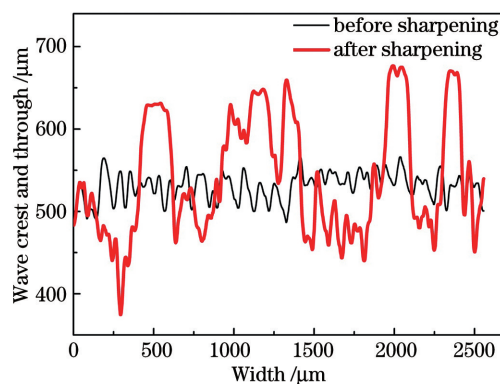


图6 青铜基金刚石砂轮修锐前后横截面粗糙度曲线

Fig. 6 Cross-sectional roughness curves for bronze-based diamond grinding wheel before and after sharpening

屑空间有限,砂轮的磨削性能差,有必要做进一步的修锐处理。经修锐后[图5(b)],磨粒间的青铜基体明显减少,磨粒突出砂轮表面,且有一定的容屑空间,面粗糙度 S_a 增大至 $55.41 \mu\text{m}$ 左右。另外,粗糙度曲线在一定范围内剧烈跳动,波峰与波谷错落有致呈周期性排列,平均高度差在 $181.30 \mu\text{m}$ 左右,表明修锐后砂轮表面产生了大量突出且具有周期性排布的金刚石磨粒,有利于获得均匀排列切削刃。工程中一般将磨粒凸出的高度作为衡量金刚石砂轮磨削性能的一个重要参数,合理控制这一高度是激光修锐的关键,如果修锐后的磨粒突出太高,不仅降低了砂轮几何尺寸精度,还将导致使用过程中刮伤磨削工件。

3.2 工艺参数对修锐效果的影响

图7为不同激光功率密度下修锐砂轮表面的三维形貌与磨粒损伤情况。由图7可知,激光功率密度为 $1.77 \times 10^{11} \text{ W/cm}^2$ 时,磨粒突出高度较小,基体表面无黑化,面粗糙度 S_a 为 $45.08 \mu\text{m}$ 左右,相

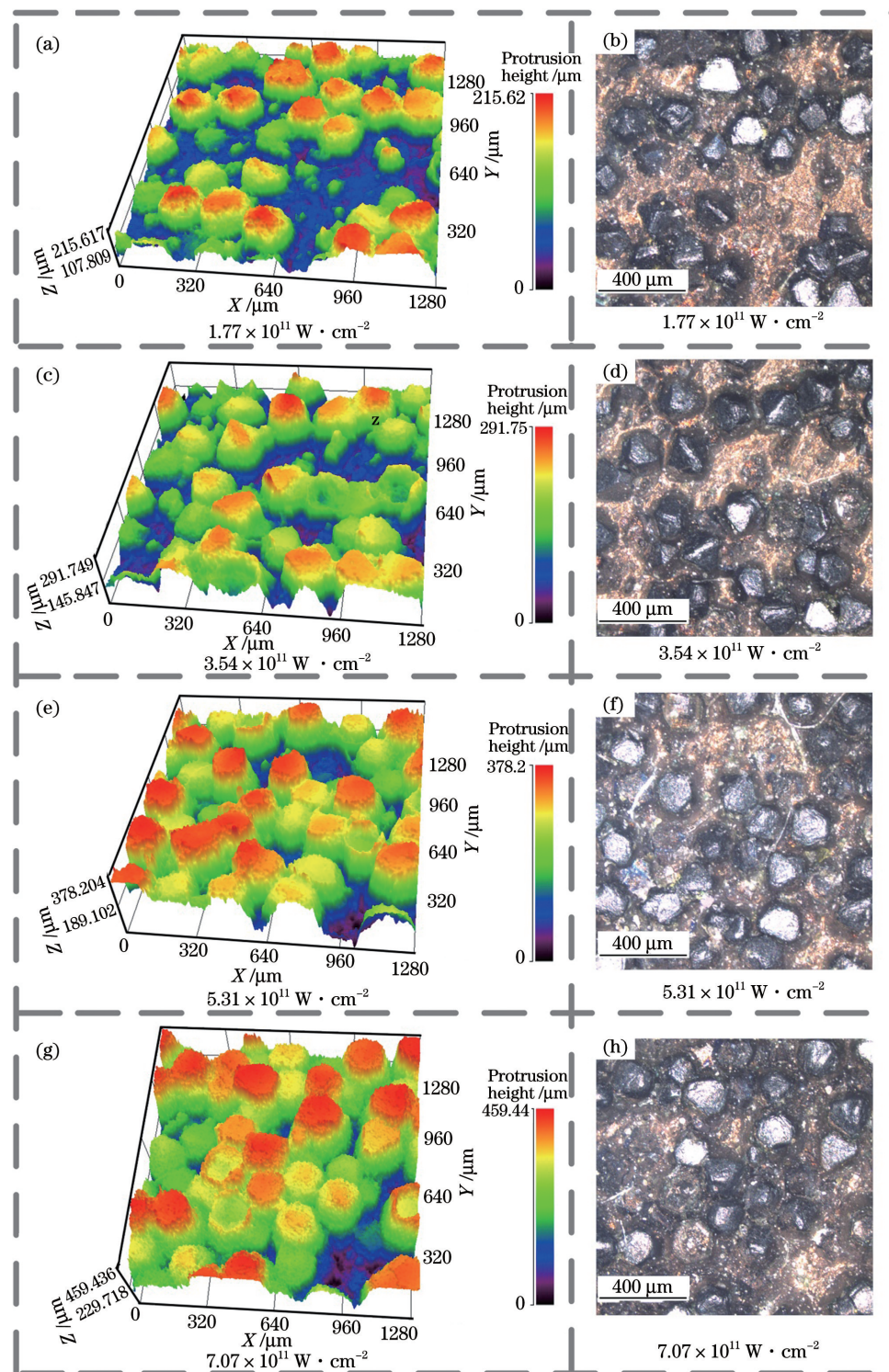


图7 不同功率密度修锐砂轮表面的三维形貌与磨粒损伤。(a)(c)(e)(g)磨粒突出高度云图;(b)(d)(f)(h)表面微观形貌
Fig. 7 Three-dimensional morphology and abrasive grain damage of grinding wheel surface under different power densities.

(a)(c)(e)(g) Cloud images of abrasive grain protrusion height; (b)(d)(f)(h) surface microtopography

比原始面粗糙度($29.78 \mu\text{m}$)变化较小,表明此时功率密度偏小,仅可微量去除青铜基体,不能形成有效的切削刃,修锐效果不理想;当功率密度增至 $3.54 \times 10^{11} \text{ W/cm}^2$ 时,面粗糙度提高至 $53.52 \mu\text{m}$,青铜基体被有效去除并形成一定数量的凹坑,大量

的金刚石磨粒裸露出砂轮表面形成微切削刃。由于此时激光功率密度较高于青铜基体损伤阈值,但尚未达到金刚石磨粒损伤阈值,使得青铜基体在有效去除的同时,金刚石磨粒能够较好地保持完整的形态,且未观察到明显的黑化现象。若进一步提高功

率密度至 $5.31 \times 10^{11} \sim 7.07 \times 10^{11} \text{ W/cm}^2$, 此时功率密度均高于基体与磨粒的损伤阈值, 青铜基体被过量去除, 单个金刚石磨粒裸露表面变得平坦 [图 7(e)和(g)], 金刚石磨粒间的青铜基体出现黑色碳化层。此时由于功率密度过高, 金刚石磨粒受到不同程度的损伤, 加之高重复频率高能脉冲的能量积累效应, 在一定程度上存在轻微的热损伤与碳化, 不适合修锐。

图 8 为功率密度为 $3.54 \times 10^{11} \text{ W/cm}^2$ 时, 低重复频率与高重复频率条件下的砂轮表面的微观形貌。

貌与磨粒损伤情况, 由图 8 可知, 当激光功率为 5 W、脉冲重复频率为 200 kHz 时, 青铜基体定量去除, 砂轮表面磨粒保留完好, 碳化程度较轻, 其主要去除机制为气化去除。在激光峰值功率密度保持不变, 同时增加激光功率与脉冲重复频率的情况下, 同样实现了较好的修锐效果(激光功率为 15 W, 脉冲重复频率为 600 kHz), 但在高重复频率的激光辐照下, 受高重复频率热积累效应影响^[26-27], 砂轮表面金刚石磨粒出现了微量损伤现象, 碳化程度有加重趋势。

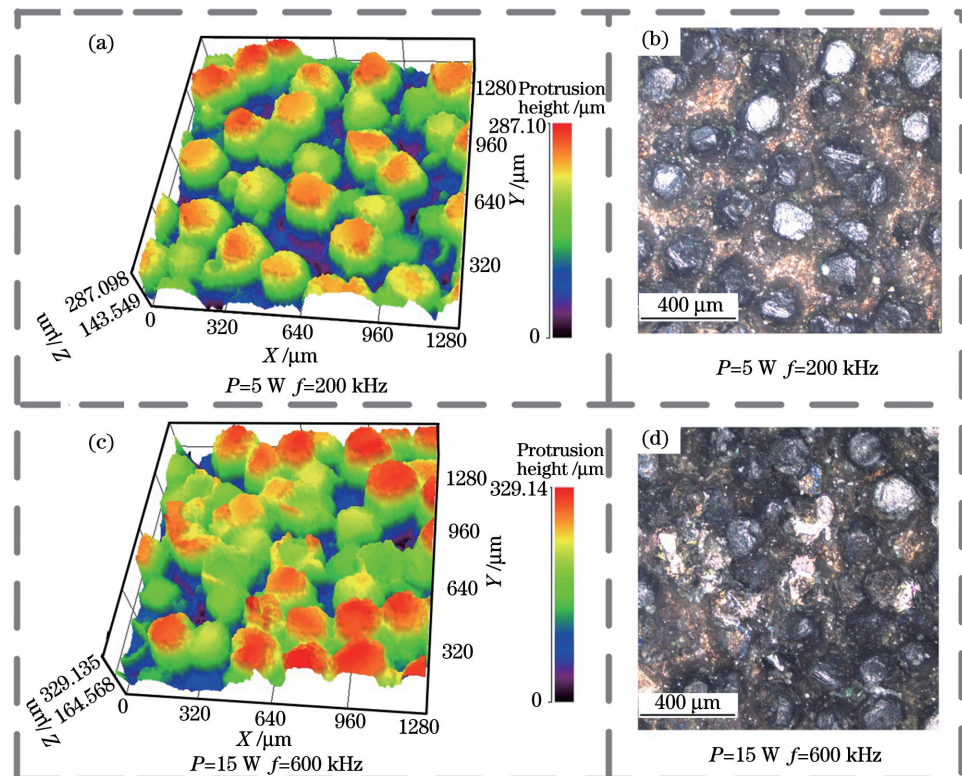


图 8 重复频率对修锐效果的影响。(a) 低重复频率;(b) 高重复频率

Fig. 8 Effect of repetition frequency on sharpening. (a) Low repetition frequency; (b) high repetition frequency

图 9 为脉冲重复频率 400 kHz, 功率密度 $3.54 \times 10^{11} \text{ W/cm}^2$, 不同扫描次数修锐砂轮表面三

维形貌。由图 9 可知, 随扫描次数的增加, 砂轮表面粗糙度显著增加, 单个金刚石磨粒表面逐渐变得平

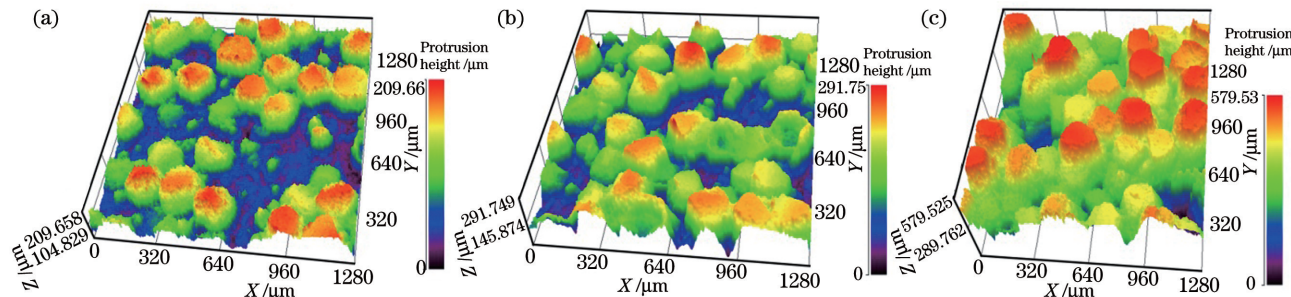


图 9 不同扫描次数修锐砂轮表面三维形貌。(a) 50 次;(b) 100 次;(c) 150 次

Fig. 9 Three-dimensional morphology of grinding wheel surface with different scanning times. (a) 50 times; (b) 100 times; (c) 150 times

整,底部逐渐裸露。扫描次数越高,青铜基体去除量越大。当扫描次数增加至100次时,磨粒突出高度约为其粒径的1/3左右,且底部仍有一定数量的青铜基体包覆。当扫描次数增加至150次时,青铜基体去除量过大,使得磨粒突出高度过高,底部不能被青铜基体有效包覆,仅浮于砂轮表面,可能导致使用过程中磨粒剥落,降低砂轮使用寿命。

4 结 论

本文利用皮秒绿激光对青铜金刚石砂轮进行了修锐试验研究。脉宽为10 ps、重复频率为400 kHz条件下,青铜基体与金刚石磨粒的损伤阈值分别为 $1.23 \times 10^9 \text{ W/cm}^2$ 和 $3.71 \times 10^{11} \text{ W/cm}^2$,两者相差两个数量级,这对青铜基体的选择性微量去除与选取工艺参数是有利的。

本文探究了青铜金刚石砂轮的皮秒激光损伤特性,相比于传统连续或短脉冲激光,皮秒激光在很大程度上减少了金刚石磨粒的碳化。如果选取合适的峰值功率密度,即使在高重复频率下,金刚石磨粒也不易碳化,无明显的热作用痕迹。

激光功率密度对修锐效果起主要作用,在激光功率一定时,可通过调整扫描次数,实现砂轮表面青铜基体的定量去除。当功率密度一定时,等比例增大激光功率与重复频率,虽然可以达到较好的修锐效果,但热积累效应逐渐增强,易导致碳化。

参 考 文 献

- [1] Li M, Yuan J L, Wu Z, et al. Progress in ultra-precision machining methods of complex curved parts [J]. Journal of Mechanical Engineering, 2015, 51(5): 178-191.
- [2] Chen G Y, Zhu Z C, Yin J, et al. Experiment on ablation threshold of single-crystal diamond produced by femtosecond laser processing [J]. Chinese Journal of Lasers, 2019, 46(4): 0402001.
- [3] Chen G Y, Xie X Z, Li L J, et al. Superabrasive wheels dressing and new development of laser dressing [J]. Diamond & Abrasives Engineering, 2002, 22(2): 8-12.
- [4] Feng K M, Zhao J Z, Xing B. Review and the prospect of dressing technology of superhard abrasive grinding wheel [J]. Ordnance Material Science and Engineering, 2019, 42(2): 115-121.
- [5] Deng H, Chen G Y, Zhou C, et al. Pulsed laser tangential profiling and radial sharpening of bronze-bonded diamond grinding wheels [J]. Chinese Journal of Lasers, 2014, 41(11): 1103003.
- [6] Wegener K, Hoffmeister H W, Karpuschewski B, et al. Conditioning and monitoring of grinding wheels [J]. CIRP Annals, 2011, 60(2): 757-777.
- [7] Deng H, Chen G Y, Zhou C, et al. Status and prospect of laser truing and dressing technique for superabrasive grinding wheels [J]. High Power Laser and Particle Beams, 2014, 26(7): 079002.
- [8] Yu J W, He L H, Huang S, et al. State-of-the-art of electrical discharge dressing technology for superabrasive grinding wheel [J]. China Mechanical Engineering, 2015, 26(16): 2254-2262.
- [9] Hosokawa A, Ueda T, Yunoki T. Laser dressing of metal bonded diamond wheel [J]. CIRP Annals, 2006, 55(1): 329-332.
- [10] Ding W F, Li H N, Zhang L C, et al. Diamond wheel dressing: a comprehensive review [J]. Journal of Manufacturing Science and Engineering, 2017, 139(12): 121006.
- [11] Zahedi A, Tawakoli T, Akbari J, et al. Conditioning of vitrified bond CBN grinding wheels using a picosecond laser [J]. Advanced Materials Research, 2014, 1017: 573-579.
- [12] Chen G Y, Cai S, Zhou C. On the laser-driven integrated dressing and truing of bronze-bonded grinding wheels [J]. Diamond and Related Materials, 2015, 60: 99-110.
- [13] Guo X G, Zhai C H, Jin Z J, et al. The study of diamond graphitization under the action of iron-based catalyst [J]. Journal of Mechanical Engineering, 2015, 51(17): 162-168.

- 郭晓光, 翟昌恒, 金洙吉, 等. 铁基作用下的金刚石墨化研究[J]. 机械工程学报, 2015, 51(17): 162-168.
- [14] Deng H, Deng Z H, Li S C. The grinding performance of a laser-dressed bronze-bonded diamond grinding wheel [J]. The International Journal of Advanced Manufacturing Technology, 2017, 88(5/6/7/8): 1789-1798.
- [15] Qin X Y, Huang T, Xiao R S. Periodic microstructure on Ti surface induced by high-power green femtosecond laser [J]. Chinese Journal of Lasers, 2019, 46(10): 1002006.
秦晓阳, 黄婷, 肖荣诗. 高功率绿光飞秒激光诱导产生钛表面周期性微结构[J]. 中国激光, 2019, 46(10): 1002006.
- [16] Wei C, Ma Y P, Han Y, et al. Femtosecond laser processing of ultrahard materials [J]. Laser & Optoelectronics Progress, 2019, 56(19): 190003.
魏超, 马玉平, 韩源, 等. 飞秒激光加工超硬材料的研究进展[J]. 激光与光电子学进展, 2019, 56(19): 190003.
- [17] Chen M, Zhang F L, Ouyang C D, et al. Research advance on mechanism of micro machining of diamond materials by pulsed laser [J]. Superhard Material Engineering, 2014, 26(1): 15-20.
陈梦, 张凤林, 欧阳承达, 等. 脉冲激光微细加工金刚石机理的研究进展[J]. 超硬材料工程, 2014, 26(1): 15-20.
- [18] Ji L F, Ling C, Li Q R, et al. Research progress and development of industrial application of picosecond laser processing [J]. Journal of Mechanical Engineering, 2014, 50(5): 115-126.
季凌飞, 凌晨, 李秋瑞, 等. 皮秒激光工程应用研究现状与发展分析[J]. 机械工程学报, 2014, 50(5): 115-126.
- [19] Dold C, Transchel R, Rabiey M, et al. A study on laser touch dressing of electroplated diamond wheels using pulsed picosecond laser sources [J]. CIRP Annals, 2011, 60(1): 363-366.
- [20] Zhang J, Zhang J C, Zhang Q M, et al. Experimental study and design of dual-wavelength coaxial hybrid laser welding system [J]. Chinese Journal of Lasers, 2017, 44(6): 0602007.
- 张健, 张津超, 张庆茂, 等. 双波长激光束同轴复合焊接系统设计与实验研究[J]. 中国激光, 2017, 44(6): 0602007.
- [21] Zhao Y, Feng A X, Yang H H, et al. Effects of laser texture process on infrared laser absorptivity of copper surface [J]. Surface Technology, 2018, 47(9): 57-64.
赵莹, 冯爱新, 杨海华, 等. 激光织构工艺对铜表面红外激光吸收率的影响[J]. 表面技术, 2018, 47(9): 57-64.
- [22] Cai S, Chen G Y, Zhou C. Research and application of surface heat treatment for multipulse laser ablation of materials [J]. Applied Surface Science, 2015, 355: 461-472.
- [23] Li Y Y, Zhang W Y, Liu Z, et al. Cumulative effect of thin film laser damage under S-on-1 measurement mode [J]. Laser Technology, 2018, 42(1): 39-42.
李玉瑶, 张婉怡, 刘喆, 等. S-on-1 测量方式下薄膜激光损伤的累积效应[J]. 激光技术, 2018, 42(1): 39-42.
- [24] Dong J N, Fan J, Wang H Z, et al. Research progress in laser damage of high reflective optical thin films [J]. Chinese Optics, 2018, 11(6): 931-948.
董家宁, 范杰, 王海珠, 等. 高反射光学薄膜激光损伤研究进展[J]. 中国光学, 2018, 11(6): 931-948.
- [25] Wang T, Zhao Y A, Huang J B, et al. Accumulation effect of multi-shot laser-induced damage to optical coatings [J]. Acta Photonica Sinica, 2006, 35(6): 859-862.
王涛, 赵元安, 黄建兵, 等. 多脉冲激光作用下光学薄膜损伤的累积效应[J]. 光子学报, 2006, 35(6): 859-862.
- [26] Zhang J, Chen Z W, Li Z Y, et al. Morphology and magnetic properties of grain-oriented steel scribed using different picosecond lasers [J]. Applied Physics A, 2020, 126(5): 1-11.
- [27] Wang T F, Tang W, Shao J F, et al. Analysis of temperature and damage characteristics of HgCdTe crystal on repetition frequency of CO₂ laser [J]. Chinese Journal of Lasers, 2015, 42(2): 0206006.
王挺峰, 汤伟, 邵俊峰, 等. 高重复频率CO₂激光重复频率大小对HgCdTe晶体温升及损伤特性影响分析[J]. 中国激光, 2015, 42(2): 0206006.

Damage Law and Mechanism of Bronze-Based Diamond Grinding Wheel Sharpening with Picosecond Green Laser

Zhou Yuanhang¹, Zhang Jian^{1,2*}, Feng Aixin^{1,2}, Shang Dazhi¹, Chen Yun³, Tang Jie¹, Yang Haihua¹

¹ College of Mechanical and Electrical Engineering, Wenzhou University, Wenzhou, Zhejiang, 325035, China;

² Key Laboratory of Laser Processing Robot of Zhejiang Province, Wenzhou, Zhejiang, 325035, China;

³ Chengdu Tool Research Institute Co., Ltd., Chengdu, Sichuan, 610500, China

Abstract

Objective Bronze-based diamond grinding wheels have been widely used, and their applications have increased sharply. However, they are difficult to dress after being blunt. Traditional dressing methods, such as mechanical and electrical dressing, have the disadvantages of large loss of dressing tools, low dressing efficiency, and serious environmental pollution. The laser dressing method has significant advantages such as high efficiency, environmental protection, controllability, and wide applicability. However, if using traditional long-wavelength continuous, millisecond, or nanosecond infrared lasers, their melting/vaporization ablation mechanism can easily cause carbonization damage of the diamond abrasive grains on the surface of the grinding wheel. The short-wavelength picosecond laser has the technical advantage of “electronic state” cold processing, which can simultaneously ensure the sharpening effect and inhibit the carbonization damage of diamond abrasive grains due to high temperatures. It has significant technical advantages when dressing the grinding wheel. In this paper, the picosecond green laser was used to radially sharpen the bronze-based diamond grinding wheel. The protocols of using a picosecond green laser to sharpen the bronze-based diamond grinding wheel were explored. Moreover, selectively and quantitatively removing of the bronze matrix at the grinding wheel was achieved.

Methods Firstly, a 10 ps green laser was focused on the bronze/diamond surface, and the damage thresholds were calibrated by the S-on-1 damage measurement method. This method allowed to determine the suitable working conditions for picosecond green laser to sharpen the bronze/diamond grinding wheels. Secondly, a picosecond green laser was used to sharpen the surface of the bronze/diamond grinding wheel. Thirdly, the surface morphology and roughness were characterized using the laser confocal microscope. Finally, the effects of laser peak power density, repetition frequency, and scanning times on the sharpening effect were studied.

Results and Discussions 1) The damage thresholds of the bronze matrix and the diamond abrasive grains differed in two orders of magnitude and amounted to 1.23×10^9 W/cm² and 3.71×10^{11} W/cm², respectively (Fig. 4). The difference in damage threshold was conducive to the selective micro-removal of the bronze matrix and the selection of the sharpening process parameters. 2) The picosecond laser damage characteristics of bronze diamond grinding wheels were studied. Next, these characteristics are compared with the traditional approach using a continuous or short-pulse laser. Picosecond laser has greatly reduced the carbonization of diamond abrasive grains. If the appropriate peak power density was selected, the diamond abrasive grains were not easy to be carbonized even at high repetition frequency, there was no obvious heat trace. 3) The laser power density played a major role in the sharpening effect (Fig. 7). When the laser power was constant, adjusting the number of scans quantitatively removed the bronze matrix at the surface of the grinding wheel (Fig. 9). When the power density was constant, a proportional increase in both the laser power and repetition frequency achieved a good sharpening effect. However, the gradual accumulation of heat has increased the chances of carbonization (Fig. 8).

Conclusions In this study, the damage rules and mechanisms of bronze-based diamond grinding wheels sharpening with picosecond laser were studied. Moreover, the damage threshold of the picosecond laser ablation of the bronze matrix/diamond was quantified, and the laws of different process parameters acting at the surface of the grinding wheel were analyzed. The removal mechanism of the picosecond green laser on the bronze matrix is mainly vaporization. It allowed avoiding the carbonization of diamond abrasive grains. Even at high repetition frequencies, there was no obvious heat accumulation. The study shows that the damage threshold of the bronze matrix and diamond abrasive grains are different in two orders of magnitude. The bronze matrix can be selectively removed by

adjusting the peak power density and quantitatively removed by adjusting the number of scans. Moreover, the picosecond green laser is capable of ensuring the integrity of the diamond abrasive grains by selectively and quantitatively removing the bronze matrix.

Key words laser processing; picosecond laser; bronze-based diamond grinding wheel; laser sharpening; damage threshold

OCIS codes 140.3390; 140.3330